AIP | Journal of Applied Physics

Monolayers of MoS2 as an oxidation protective nanocoating material

H. Sener Sen, H. Sahin, F. M. Peeters, and E. Durgun

Citation: Journal of Applied Physics **116**, 083508 (2014); doi: 10.1063/1.4893790
View online: http://dx.doi.org/10.1063/1.4893790
View Table of Contents: http://scitation.aip.org/content/aip/journal/jap/116/8?ver=pdfcov
Published by the AIP Publishing

Articles you may be interested in

Surface oxidation energetics and kinetics on MoS2 monolayer
J. Appl. Phys. **117**, 135301 (2015); 10.1063/1.4916536

Optimal electron irradiation as a tool for functionalization of MoS2: Theoretical and experimental investigation
J. Appl. Phys. **117**, 135701 (2015); 10.1063/1.4916530

Joint first-principles/continuum calculations of electromechanical properties of MoS2 monolayer
Appl. Phys. Lett. **105**, 061910 (2014); 10.1063/1.4893360

Atomistic simulation of the electronic states of adatoms in monolayer MoS2
Appl. Phys. Lett. **104**, 141603 (2014); 10.1063/1.4870767

The pristine atomic structure of MoS2 monolayer protected from electron radiation damage by graphene
Appl. Phys. Lett. **103**, 203107 (2013); 10.1063/1.4830036

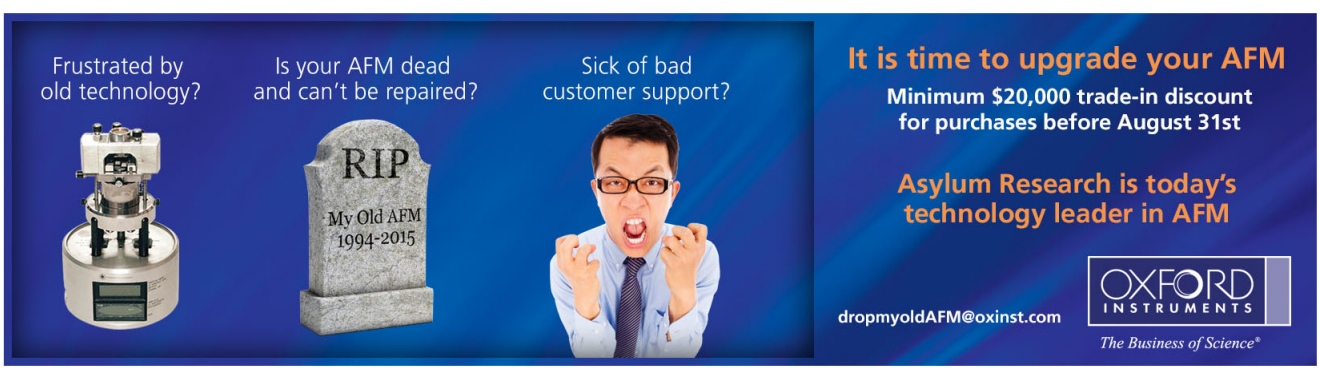

[This article is copyrighted as indicated in the article. Reuse of AIP content is subject to the terms at: http://scitation.aip.org/termsconditions. Downloaded to] IP: 139.179.2.116 On: Tue, 16 Jun 2015 14:11:18

Monolayers of MoS_2 as an oxidation protective nanocoating material

H. Sener Sen,[1] H. Sahin,[2] F. M. Peeters,[2] and E. Durgun[1,3,a)]
[1]*UNAM-National Nanotechnology Research Center, Bilkent University, Ankara 06800, Turkey*
[2]*Department of Physics, University of Antwerp, 2610 Antwerp, Belgium*
[3]*Institute of Materials Science and Nanotechnology, Bilkent University, Ankara 06800, Turkey*

(Received 3 July 2014; accepted 12 August 2014; published online 26 August 2014)

First-principle calculations are employed to investigate the interaction of oxygen with ideal and defective MoS_2 monolayers. Our calculations show that while oxygen atoms are strongly bound on top of sulfur atoms, the oxygen molecule only weakly interacts with the surface. The penetration of oxygen atoms and molecules through a defect-free MoS_2 monolayer is prevented by a very high diffusion barrier indicating that MoS_2 can serve as a protective layer for oxidation. The analysis is extended to WS_2 and similar coating characteristics are obtained. Our calculations indicate that ideal and continuous MoS_2 and WS_2 monolayers can improve the oxidation and corrosion-resistance of the covered surface and can be considered as an efficient nanocoating material. *© 2014 Author(s). All article content, except where otherwise noted, is licensed under a Creative Commons Attribution 3.0 Unported License.* [http://dx.doi.org/10.1063/1.4893790]

I. INTRODUCTION

Depending on the requirements on the functionality of an application, such as, reduction of friction forces (lubrication), passivation of chemical reactivity, and/or protection from corrosion/wear, surface coating has always been an active research area in different fields. At macroscale, a surface can be covered by different materials including paints,[1] polymers,[2] organic layers,[3–5] metals, and alloys.[6] Conventional coating materials modify the structural and physical properties of the underlying structure which can result in undesired alterations. These effects are more drastic in reduced dimensions, especially in nanoscale systems. Therefore, it is essential to find a suitable material that protects the surface without losing the desired properties. With this motivation, theoretical and experimental research on novel coating materials of a few atomic layer thickness have emerged. Being an ultra-thin, strong and light material, graphene[7] has been viewed as an ideal nanocoating material. Various metal surfaces including Ni,[8,9] Ru(0001),[10] Cu/Ni alloy,[11] Cu,[12,13] Ir(111), and Pt(111)[14] have been coated by graphene and a reduction in the oxidation of the surface was reported. It was theoretically shown that even graphene itself strongly interacts with oxygen atoms, it poses a high energy barrier for the penetration of oxygen and thus can protect the surface underneath against oxidation as long as the graphene coating is defect free.[15]

Recent advances made growth and exfoliation of single layers of lamellar materials beyond graphene also possible. Among these novel materials, two-dimensional MoS_2[16] which belongs to the family of transition metal dichalcogenides (TMD), has been of special interest for nanocoating since its bulk form is a well-known coating material at macro scale.[17–19] MoS_2 crystals are composed of vertically stacked layers with an interlayer distance of 6.5 Å (JCPDS 77-1716) interacting via Van der Waals (vdW) forces, similar to graphite.[20] The unit cell of MoS_2 consists of a Mo-layer sandwiched between two S-layers. Each of these sub-layers has a hexagonal structure in plane and S atoms are chemically bonded with the Mo atoms in a trigonal prismatic fashion. Weak interatomic interactions between its layered structures allow easy and low-strength shearing. MoS_2 can be used as solid lubricant when load carrying capacity, operating temperature, and friction are crucial parameters and liquid lubricants are impractical.[17–19] It is also shown that thin films of fullerene-like MoS_2 nanoparticles have an ultra-low friction coefficient in ambient conditions, which makes them an ideal material for tribological applications.[17] In the ultimate limit of a single layer, MoS_2 posses different optical, mechanical, and electrical properties than its bulk phase. Bulk MoS_2, for instance, is a semiconductor with an indirect band gap of 1.3 eV, whereas monolayer MoS_2 is a direct band gap semiconductor with a band gap of 1.8 eV.[21–23] New emerging properties allow single or a few-layered MoS_2 to be used in different fields such as photocatalyst,[24,25] a field effect transistor,[26,27] and photosensitive thin film for solar applications.[28,29] Although oxygen adsorption on MoS_2 monolayers[30,31] and effects of oxygen on device applications have been examined,[27] the possibility of using MoS_2 monolayers as a protective coating material against oxidation for reactive surfaces has not been considered yet.

In this work, we study the interaction of oxygen (adsorption and diffusion) with a MoS_2 monolayer for potential usage in nanocoating applications. First, we examine the adsorption of oxygen atom/molecule on MoS_2. Next, we determine the minimum energy path and the reaction barrier for lateral and vertical diffusion of oxygen through ideal and suspended MoS_2. In addition, the possible effect of the underlaying surface is taken into account by fixing the bottom S-layer. We repeat the analysis for defective MoS_2 containing various types of vacancies. Finally, the study is extended to similar structures made of monolayer WS_2.

II. METHODOLOGY

In this study, we performed first-principles, spin-polarized calculations within density functional theory[32,33] using

a)Electronic mail: durgun@unam.bilkent.edu.tr

 © Author(s) 2014

[This article is copyrighted as indicated in the article. Reuse of AIP content is subject to the terms at: http://scitation.aip.org/termsconditions. Downloaded to] IP: 139.179.2.116 On: Tue, 16 Jun 2015 14:11:18

the Vienna *ab initio* simulation package (VASP).[34,35] Exchange-correlation energy was expressed by the generalized gradient approximation[36] including vdW correction and the projector augmented wave (PAW) potential[37] is used with kinetic energy cutoff of 500 eV. In order to minimize the interaction of adsorbed atoms/molecules with their replica in the neighboring cells, the calculations were carried out in a 4×4 supercell with 15 Å vacuum spacing in the vertical direction. In the self-consistent potential and total energy calculations, the Brillouin zone of the supercell was sampled in the **k**-space using $5 \times 5 \times 1$ mesh points.[38] All structures were relaxed using the Kosugi algorithm[39] with simultaneous minimization of the total energy and the interatomic forces. The convergence for the total energy was set to 10^{-5} eV, and the maximum residual force allowed on each atom was fixed at 10^{-2} eV/Å.

The energetics of oxygen vertical diffusion were calculated by forcing it to penetrate through the MoS_2 layer. The minimum energy path was determined by 0.2 Å vertical displacement of O/O_2. At each step, the lateral coordinates of oxygen were relaxed while the perpendicular coordinate was kept fixed. MoS_2 is considered to be free-standing where all atoms were fully relaxed except specific Mo atoms which were kept fixed to prevent the displacement of the suspended layer. When necessary, the energy barrier of the reaction paths was calculated by using the nudged-elastic band approach.[40]

III. OXYGEN ADSORPTION ON MoS_2 MONOLAYER

In order to understand the interaction of oxygen with MoS_2, we start with the adsorption of a single oxygen atom on the MoS_2 surface. We consider a 4×4 supercell to avoid artificial O-O interaction and consider three possible adsorption sites, namely hollow (H), bridge (B), and top (T) as shown in Fig. 1(a). Our results indicate that independent of the initial configuration the O atom always prefers the top site and binds to a sulfur atom (S_t) on top (Figs. 1(a) and 1(c)). The bond length (d_{S-O}) is calculated as 1.48 Å indicating a strong interaction between O and S atoms. The ground state of the system is non-magnetic with zero total magnetic moment. The adsorption energy (E_b) of O atom (and also O_2 molecule) on MoS_2 is given by

$$E_b = E_T(MoS_2) + E_T(O_x) - E_T(MoS_2 + O_x), \quad (1)$$

where E_T (MoS_2), E_T (O_x), and E_T ($MoS_2 + O_x$) are the total energy of fully optimized bare MoS_2 (4×4 supercell), oxygen atom (x = 1) or molecule (x = 2), and MoS_2-O_x system, respectively. All energies are calculated within the same supercell for the sake of comparison. Using Eq. (1), E_b of a single O atom is obtained as 3.93 eV indicating a strong covalent character. The inclusion of vdW correction in our calculations does not make any significant changes without modifying the d_{S-O} but it only slightly increases E_b by 20 meV. Fig. 2(b) displays the total and projected density of states before and after O atom adsorption. This analysis shows that 2*p* orbitals of O mix with 3*p* orbitals of S to form a strong bond. Upon adsorption, initially three-coordinated S_t atom becomes four-coordinated, which is not unexpected as sulfur can have four-bonds in a tetragonal manner in several compounds including ZnS and H_2SO_4. The difference in charge density $[\rho(MoS_2 + O) - \rho(MoS_2) + \rho(O)]$ indicates that adsorption locally affects the electron distribution (Fig. 2(a)). The O atom takes only the charge from S_t but all the other atoms are not significantly affected. We quantify the charge exchange by using a Bader analysis.[41] When ideal MoS_2 is analyzed, the net charge on Mo and S atoms is +1.05 e and −0.53 e, respectively. As a consequence of the adsorption, S_t donates electrons to O and becomes positively charged. The net charge on O and S_t becomes −1.15 e and +0.60 e, respectively. The charge exchange is of the same order as the electronegativities (χ) of the considered atoms where $\chi_O > \chi_S > \chi_{Mo}$. The net charge on all the other atoms remains the same confirming the localized affect obtained by the difference charge density analysis. Accordingly, additional O atom(s) can bind to a neighboring S atom(s) in a similar manner. For instance, we try out a second O atom that binds to the S atom adjacent to S_t on top with a slightly lower $E_b = 3.52$ eV. Our calculations also indicate that the substitution of S with O atoms is an endothermic process and requires high energy. The reaction barrier is calculated as 4.5 eV for replacing single S with O atom.[42]

Next, we study the lateral diffusion of the O atom on the MoS_2 surface. The minimum energy path and corresponding energy variation is shown in Fig. 1. Our analysis reveals that

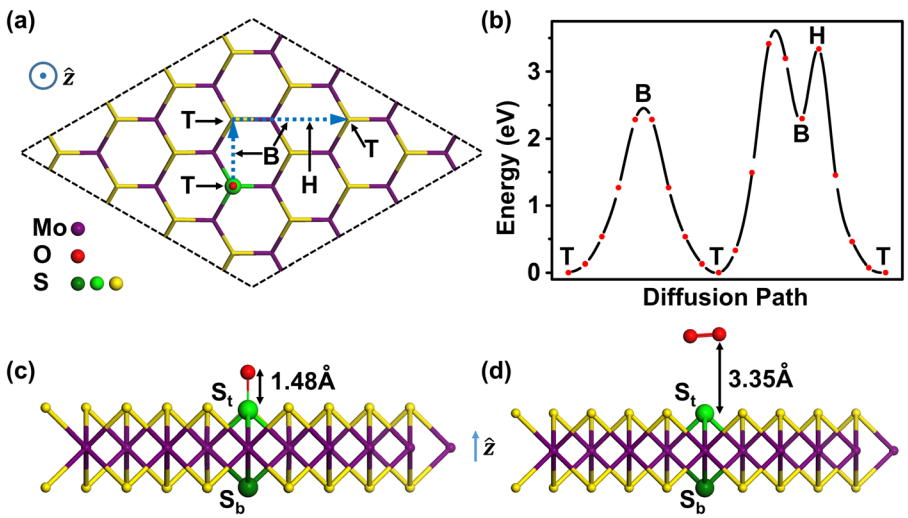

FIG. 1. (a) Top view of atomic oxygen adsorption. The adsorption cites are indicated by T (on top of S atom), B (in between two neighboring S atoms), and H (center of the hexagon). The lateral diffusion path is shown by dashed, blue arrows. (b) The energetics of oxygen lateral diffusion. Side view of (c) atomic and (d) molecular oxygen adsorption on MoS_2 monolayer. z-axes is normal to the surface. Purple, red, and yellow spheres represent Mo, O, and S atoms, respectively. The S atoms interacting with oxygen is label as S_t (top layer) and S_b (bottom layer) and are represented with light and dark green spheres, respectively.

[This article is copyrighted as indicated in the article. Reuse of AIP content is subject to the terms at: http://scitation.aip.org/termsconditions. Downloaded to] IP: 139.179.2.116 On: Tue, 16 Jun 2015 14:11:18

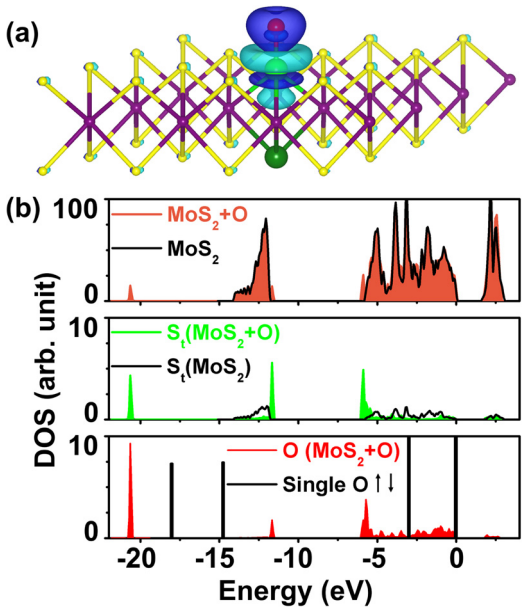

FIG. 2. (a) The difference charge density plot upon oxygen atom adsorption and (b) corresponding total density of states (top panel) and projected density of states on S_t (middle panel) and O (bottom panel) atoms before (solid black line) and after (coloured region) adsorption.

bridge (B) and hollow (H) cites are metastable and the O atom stays only at the top (T) site. The diffusion barrier for a single atomic O is high for all directions and calculated as 2.28 eV for T → B, 3.41 eV for T → B → H, and 3.34 for T → H.

In contrast to single O adsorption, the interaction of an O_2 molecule with MoS_2 is weak and it can only be physisorbed. Similar to the O atom case, we try various adsorption cites but we find that O_2 does not chemically bind and stays at a physisorption distance of ~3.40 Å as shown in Fig. 1(c). Using Eq. (1), E_b is calculated as 0.07 eV when vdW corrections are included. The net magnetic moment of the system is 2 μ_B indicating that O_2 is still in the triplet state. Even if the initial position of O_2 is chosen to be very close to MoS_2 with elongated O-O bond, the molecule O_2 would rather move away from the surface than bind to it. Accordingly, ideal MoS_2 does not dissociate O_2 under normal conditions and dissociation requires a high external energy.

As a final step, we consider the interaction of another O atom with the adsorbate. Interestingly, when the incoming O atom approaches the adsorbed one on top, the O-S_t bond is broken at a distance of 1.63 Å and then O_2 is formed. Afterwards, the O_2 molecule moves away from the surface as expected. However, when the incoming O approaches from the side, it first interacts with MoS_2 and binds to a nearby S atom on top. Even if these O atoms are forced to get in close proximity, they do not form an O_2 molecule once they receive charge from S atoms. The configuration where two O atoms bind to neighboring S atom is energetically 1.1 eV more favorable than the formation of O_2 molecule.

In conclusion, our results indicate that even though MoS_2 does not interact with O_2 molecules, it can be easily oxidized by atomic oxygen. However, the lateral diffusion barrier is high for adsorbed atomic O and prevents its movement on the surface; a second O atom can break the O-S bond by forming O_2 molecule.

IV. PENETRATION OF OXYGEN THROUGH MoS_2 COATING

A. Ideal MoS_2 monolayer

Clarifying the interaction of oxygen with a MoS_2 monolayer, we now address the vertical diffusion of atomic O and molecular O_2 through MoS_2. The minimum energy path and the resulting energy barriers of oxygen for vertical diffusion can reveal the possibility of using MoS_2 as a protective layer. As we are not interested in a specific reactive surface, we mainly focus on suspended MoS_2 monolayer. In this model, MoS_2 is considered to be free-standing where only specific Mo atoms are fixed to prevent the displacement of the suspended layer and all other atoms are fully relaxed. This approach is expected to work for the cases where the surface-MoS_2 interaction is not very strong and MoS_2 has some flexibility to bend. For instance, Topsakal *et al.*[15] calculated the diffusion barrier of oxygen through a graphene monolayer as 5.98 and 5.93 eV with and without an underlaying Al (111) surface which indicates that the considered model yields realistic results.

We start with the penetration of atomic oxygen though suspended MoS_2. Snapshots of the minimum energy path and corresponding energy variation are represented in Fig. 3(a). The path starts from the adsorption site where O atom is on top of S_t. The O atom is then manually pushed vertically in the z-direction with 0.2 Å increments. At each step, the lateral coordinates of O atom are relaxed but the perpendicular coordinate is kept fixed. MoS_2 is considered to be free-standing where all atoms were fully relaxed except specific Mo atoms which were pinned to prevent displacement of the suspended layer. As can be noticed from the snapshots, the vertical movement of O atom pushes the S_t and S_b atoms and MoS_2 is bent until O reaches the Mo-layer in the middle. The strong S-O interaction discussed in the previous section makes O penetration difficult yielding a high diffusion energy barrier (ΔE) which is calculated to be 13.94 eV. Notice that ΔE is significantly larger than the reported barrier for suspended graphene (5.98 eV).[15]

When the surface-MoS_2 interaction gets strong, the sulfur atoms at the bottom layer can bind covalently with the underlaying surface and are no longer free to move. In such cases, it is reasonable to fix the bottom sulfur layer of MoS_2 while allowing other atoms to relax. Completely free and fixed bottom layer can model the two extreme cases and can set upper and lower boundaries for the oxygen diffusion barrier. When the bottom S-layer remains fixed, it prevents the MoS_2 from bending during atomic O penetration. Therefore, the only possible diffusion path of the O atom is to replace S_t as shown in Fig. 3(b) and this significantly reduces ΔE and calculated to be 4.88 eV. On the other hand, this time minimum energy path reveals a second energy barrier which emerges mainly due to the O-S_t bond breaking during diffusion and it is calculated as 4.13 eV. Although ΔE is reduced, two energy barriers still indicate the resistance of MoS_2

[This article is copyrighted as indicated in the article. Reuse of AIP content is subject to the terms at: http://scitation.aip.org/termsconditions. Downloaded to] IP: 139.179.2.116 On: Tue, 16 Jun 2015 14:11:18

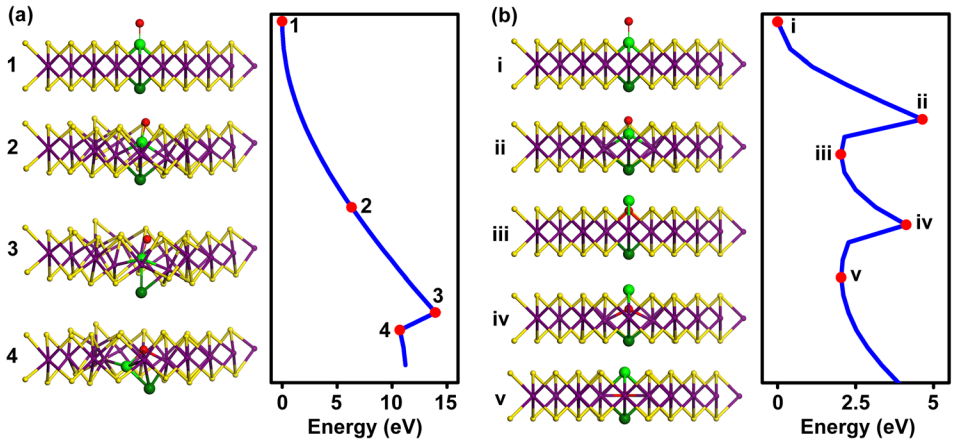

FIG. 3. The minimum energy path of an atomic oxygen penetration through an ideal MoS_2 monolayer. (a) MoS_2 is considered to be free-standing where only specific Mo atoms are fixed to prevent the displacement of the suspended layer and all other atoms are fully relaxed (b) The bottom sulfur layer of MoS_2 is kept fixed while allowing other atoms to relax.

against oxygen diffusion. We claim that this case results in a lower bound, because, although the substrate can prevent the bottom S-layer to move downwards to some extent, there will still be a bending of the MoS_2 layer. Accordingly, ΔE is expected to be in the range of 4.88–13.94 eV as the considered models set lower and upper limits for ΔE.

Next, we consider vertical diffusion of O_2 molecule keeping the same approach followed in the atomic O case. Snapshots of the minimum energy path and corresponding energy variation are represented in Fig. 4(a). The path starts with the adsorption site obtained in the previous section and then O_2 molecule is forced to move vertically down by steps of 0.2 Å. Only the vertical coordinate of one of the O atoms is kept fixed and the other one is free to move. For the suspended MoS_2 case, when O_2 starts to approach MoS_2 monolayer, it rotates and becomes perpendicular to the surface. Throughout the diffusion path, O_2 pushes S_t and S_b until it expels them. ΔE is high and is calculated to be 11.69 eV. The total energy of the system reduces when S_b is expelled and S_t substitutes it and the vacant S_t is filled by oxygen.

As discussed in the atomic O case, free-standing MoS_2 is an extreme case and thus S_b may not be pulled of from the monolayer when there is an underlying surface (Fig. 4(b)). To include this effect, once again we fix the bottom sulfur layer of MoS_2 while allowing other atoms to relax. In this path, once again the O_2 molecule approaches the surface in the vertical direction and pushes S_t but this time S_b is pinned, and the O_2 molecule dissociates and one of the O atom replaces S_t while the remaining one forms a new bond with S_t. This diffusion path gives rise to three energy barriers which are calculated to be 3.94, 1.98, and 3.63 as shown in Fig. 4(b).

Our results indicate that the calculated ΔE is high enough to prevent the penetration of oxygen atom/molecule through ideal MoS_2. The strong and directional bonding between O and S atoms makes the vertical diffusion very difficult. Oxygen cannot penetrate though MoS_2 without expelling or replacing the S atom(s) and these both require high energies. ΔE depends on the MoS_2-surface interaction and is higher when MoS_2 is free to bend and is therefore maximum for the suspended case.

B. MoS_2 monolayer with defects

The above analysis was limited to continuous and defect-free MoS_2. In the literature, various type of defects in MoS_2 have been reported[43,44] and thus a MoS_2 coating may contain vacancies in practice. Among possible defects, we consider three vacancy types, namely single sulfur (S_v), single Mo (Mo_v), and single Mo and two sulfur ($(Mo+2S)_v$) atom(s) vacancies as shown in Fig. 5(a) and we examine O/O_2 adsorption and vertical diffusion. The obtained results are summarized in Table I. Introducing a vacancy changes the adsorption profile and the corresponding structures upon O and O_2 adsorption are shown in Figs. 5(b) and 5(c). When there is a S-vacancy in the monolayer (S_v or $(Mo+2S)_v$), the O atom fills the vacancy, substituting the missing S and

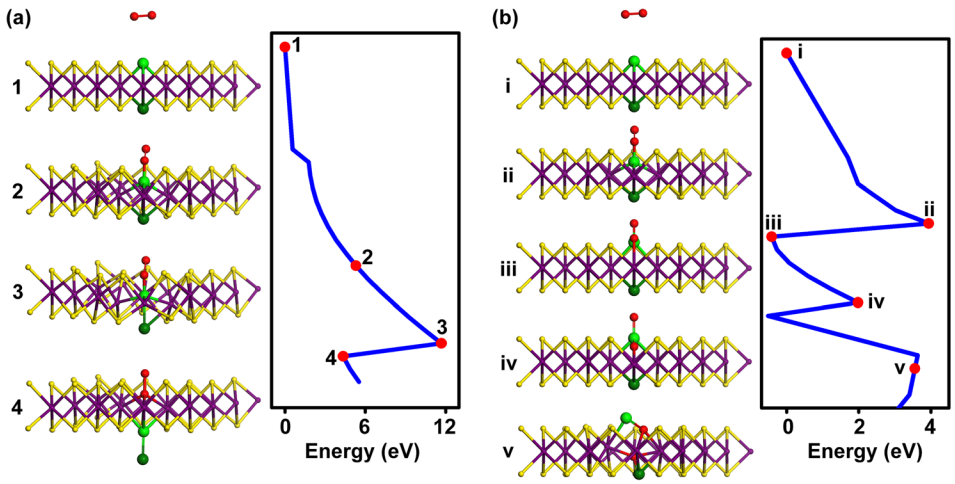

FIG. 4. The minimum energy path of oxygen molecule penetration through an ideal MoS_2 monolayer. (a) MoS_2 is considered to be free-standing where only specific Mo atoms are fixed to prevent the displacement of the suspended layer and all other atoms are fully relaxed. (b) The bottom sulfur layer of MoS_2 is kept fixed while allowing other atoms to relax.

[This article is copyrighted as indicated in the article. Reuse of AIP content is subject to the terms at: http://scitation.aip.org/termsconditions. Downloaded to] IP: 139.179.2.116 On: Tue, 16 Jun 2015 14:11:18

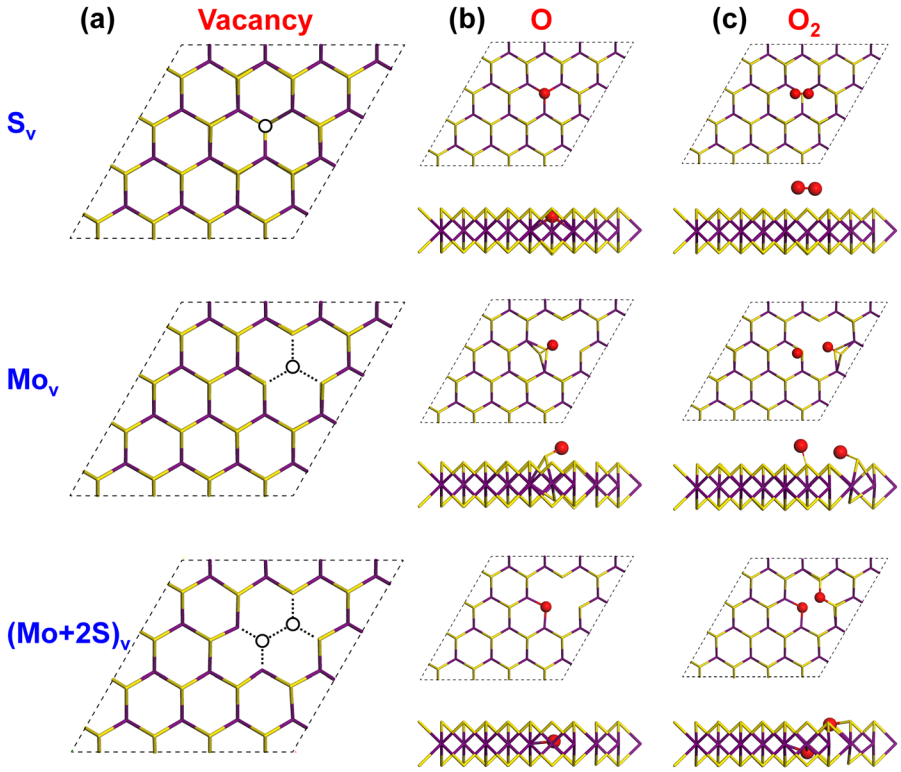

FIG. 5. The structure of MoS_2 with (a) single sulfur (S_v), single Mo (Mo_v), and single Mo and two sulfur $(Mo+2S)_v$ vacancies. (b) Side and top view of oxygen atom and (c) oxygen molecule adsorption on defected MoS_2.

binds to Mo.[31] Using Eq. (1) (considering the total energy of defected MoS_2), E_b is calculated as 7.40 and 7.76 eV for S_v and $(Mo+2S)_v$, respectively. In the case of Mo_v, the O atom binds to S atom with E_b of 4.07 eV which is almost equal to the ideal MoS_2 case. The O_2 molecule weakly interacts with MoS_2 when there is S_v yielding only 0.12 eV binding energy when vdW correction is included. When there is Mo_v or $(Mo+2S)_v$, O_2 molecule still weakly interacts with MoS_2. However, this state is metastable and O_2 can easily dissociate once overcoming a small energy barrier and then O atoms bind to S_t atoms with a high binding energy.

For each type of vacancy, we examine the vertical diffusion of atomic and molecular oxygen separately following the same methodology. The path starts from the adsorption geometry as shown in Figs. 5(b) and 5(c) then O/O_2 is pushed vertically with 0.2 Å increments while relaxing the system at each step except for the z-coordinate of oxygen. The minimum energy path and the corresponding energy barriers are illustrated in Fig. 6. Our analysis indicates that

TABLE I. The binding energy E_b, the binding energy E_b^{VdW} with van der Waals correction, and vertical diffusion energy barrier ΔE are reported for O atom and O_2 molecule on defected and defect-free MoS_2.

	Vacany	E_b (eV)	E_b^{VdW} (eV)	ΔE (eV)
O atom	…	3.93	4.07	4.88–13.94
	S	7.24	7.40	7.40
	Mo	3.89	4.02	0.13, 0.40
	Mo + 2S	7.61	7.76	4.00
O_2 molecule	…	0.00	0.07	3.94–11.69
	S	0.00	0.12	4.32
	Mo	1.70	1.92	0.23, 0.38
	Mo + 2S	5.16	5.51	2.49

ΔE significantly decreases when MoS_2 contains defects. The effect is less significant for S_v where ΔE becomes 7.80 and 4.32 eV for O and O_2, respectively. For the other types of vacancy, ΔE drastically reduces and is calculated to be even less than 0.5 eV for Mo_v. To the best of our knowledge, Mo_v is not a common defect type and has yet not been found experimentally. We conclude that vacant formation weakens oxidation protection of the MoS_2 coating but still blocks oxygen diffusion to some extend. Therefore, multiple layers of MoS_2 coating should be considered for efficient protection.

C. Alternative TMD structures: Monolayer of WS_2

As our results indicate that strong S-O interaction is a critical parameter to determine the oxidation resistance, we consider WS_2, whose bulk form is used in macro scale coating, as an alternative material in the class of TMDs. Two-dimensional WS_2 has also been synthesized and its novel properties has been revealed.[16,45] WS_2 has a similar crystal structure as MoS_2 and is composed of vertically stacked layers with an interlayer distance of 6.24 Å. We start with the oxidation of WS_2 and obtain similar results as found for MoS_2. While the O atom is chemisorbed on WS_2 forming a strong bond with S ($E_b = 3.95$ eV, $d_{S-O} = 1.48$ Å), O_2 molecule weakly interacts with WS_2 ($E_b = 0.05$ eV, $d_{S-O} > 3$ Å). Fig. 1 roughly represents the optimized structures.

The penetration of O/O_2 is studied using similar methodology and minimum energy paths are found to resemble those for the case of MoS_2. For ideal, suspended WS_2, ΔE is calculated as 9.26 and 7.26 eV for O atom and O_2 molecule, respectively. Note that ΔE is smaller than those obtained for ideal MoS_2. For WS_2, however, the S-O interaction is very strong, it is slightly weaker than the one for MoS_2 and this can explain the reduction in the diffusion barrier. ΔE is still

[This article is copyrighted as indicated in the article. Reuse of AIP content is subject to the terms at: http://scitation.aip.org/termsconditions. Downloaded to] IP: 139.179.2.116 On: Tue, 16 Jun 2015 14:11:18

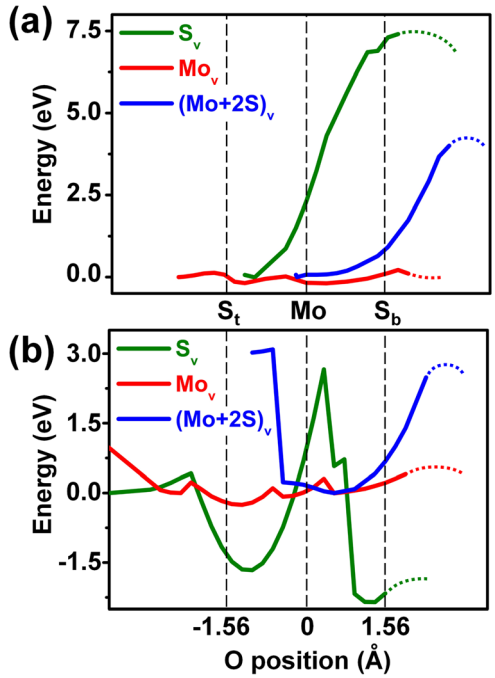

FIG. 6. The minimum energy path of (a) atomic and (b) molecular oxygen vertical diffusion through MoS_2 with defects. The vertical dashed lines indicate the position of the Mo- and S-layers in MoS_2.

very high to prevent penetration of atomic and molecular oxygen and indicates that WS_2, and similar systems in the same class can also be considered as protective nanocoating material.

V. CONCLUSIONS

In conclusion, we showed that (1) while MoS_2 weakly interacts with molecular oxygen, it can be easily oxidized by oxygen atoms, (2) continuous and defect-free MoS_2 can serve as an ideal nanocoating material which can protect the underlying surface from oxidation. The strong sulfur-oxygen interaction makes penetration of oxygen atom/molecule through the monolayer very difficult which gives rise to high energy barriers, and (3) the vertical diffusion barrier reduces when vacancies are introduced but is still high enough for most of the cases to resist against oxygen penetration. A similar trend is obtained for WS_2 which indicates that the results can be generalized for the systems in the same class.

ACKNOWLEDGMENTS

This work was supported by the bilateral project between TUBITAK (through Grant No. 113T050) and Flemish Science Foundation (FWO-Vl). The calculations were performed at TUBITAK ULAKBIM, High Performance and Grid Computing Center (TR-Grid e-Infrastructure). E.D. acknowledges support from Bilim Akademisi—The Science Academy, Turkey under the BAGEP program. H.S. is supported by an FWO Pegasus-long Marie Curie Fellowship.

[1]D. M. Merkula, P. D. Novikov, V. N. Ivanenkov, V. V. Sapozhnikov, and Y. I. Lyakhin, Oceanology **14**, 299300 (1974).
[2]M. I. Redondo and C. B. Breslin, Corros. Sci. **49**, 1765–1776 (2007).
[3]J. E. Gray and B. Luan, J. Alloy Compd. **336**, 88–113 (2002).
[4]B. V. A. Rao, M. Y. Iqbal, and B. Sreedhar, Corros. Sci. **51**, 1441–1452 (2009).
[5]M. Stratmann, R. Feser, and A. Leng, Electrochim. Acta. **39**, 1207–1214 (1994).
[6]M. Segarra, L. Miralles, J. Diaz, H. Xuriguera, J. M. Chimenos, F. Espiell, and S. Pinol, Mater. Sci. Forum **426–432**, 3511–3516 (2003).
[7]K. Novoselov, A. K. Geim, S. Morozov, D. Jiang, M. Katsnelson, I. Grigorieva, S. Dubonos, and A. Firsov, Nature **438**, 197–200 (2005).
[8]Y. S. Dedkov, M. Fonin, U. Rudiger, and C. Laubschat, Appl. Phys. Lett. **93**, 022509 (2008).
[9]Y. S. Dedkov, M. Fonin, and C. Laubschat, Appl. Phys. Lett. **92**, 052506 (2008).
[10]B. Borca, F. Calleja, J. J. Hinarejos, A. L. V. Parga, and R. Miranda, J. Phys.: Condens. Matter. **21**, 134002 (2009).
[11]S. Chen, L. Brown, M. Levendorf, W. Cai, S. Y. Ju, J. Edgeworth, X. Li, C. W. Magnuson, A. Velamakanni, R. D. Piner, J. Kang, J. Park, and R. S. Ruoff, ACS Nano. **5**, 1321–1327 (2011).
[12]S. Gadipelli, I. Calizo, J. Ford, G. Cheng, A. R. H. Walker, and T. Yildirim, J. Mater. Chem. **21**, 16057–16065 (2011).
[13]J. Cho, L. Gao, J. Tian, H. Cao, W. Wu, Q. Yu, E. N. Yitamben, B. Fisher, J. R. Guest, Y. P. Chen, and N. P. Guisinger, ACS Nano. **5**, 3607–3613 (2011).
[14]N. A. Vinogradov, K. Schulte, M. L. Ng, A. Mikkelsen, E. Lundgren, N. Martensson, and A. B. Preobrajenski, J. Phys. Chem. C. **115**, 9568–9577 (2011).
[15]M. Topsakal, H. Sahin, and S. Ciraci, Phys. Rev. B. **85**, 155445 (2012).
[16]J. N. Coleman, M. Lotya, A. O'Neill, S. D. Bergin, P. J. King, U. Khan, K. Young, A. Gaucher, S. De, R. J. Smith, I. V. Shvets, S. K. Arora, G. Stanton, H.-Y. Kim, K. Lee, G. T. Kim, G. S. Duesberg, T. Hallam, J. J. Boland, J. J. Wang, J. F. Donegan, J. C. Grunlan, G. Moriarty, A. Shmeliov, R. J. Nicholls, J. M. Perkins, E. M. Grieveson, K. Theuwissen, D. W. McComb, P. D. Nellist, and V. Nicolosi, Science **331**, 568–571 (2011).
[17]M. Chhowalla and G. A. J. Amaratunga, Nature **407**, 164–167 (2000).
[18]C. Donnet, J. M. Martin, Th. Le Mogne, and M. Belin, Tribol. Int. **29**, 123–128 (1996).
[19]H. H. Chien, K. J. Ma, S. V. P. Vattikuti, C. H. Kuo, C. B. Huo, and C. L. Chao, Thin Solid Films. **518**, 7532–7534 (2010).
[20]K. S. Novoselov, D. Jiang, T. Booth, V. V. Khotkevich, S. M. Morozov, and A. K. Geim, Proc. Natl. Acad. Sci. U.S.A. **102**, 10451–10453 (2005).
[21]K. K. Kam and B. A. Parkinson, J. Phys. Chem. **86**, 463–467 (1982).
[22]K. F. Mak, C. Lee, J. Hone, J. Shan, and T. F. Heinz, Phys. Rev. Lett. **105**, 136805 (2010).
[23]C. Ataca, H. Sahin, and S. Ciraci, J. Phys. Chem. C **116**, 8983–8999 (2012).
[24]J. P. Wilcoxon, T. R. Thurston, and J. E. Martin, Nanostruct. Mater. **12**, 993–997 (1999).
[25]B. Abrams and J. Wilcoxon, Crit. Rev. Solid State Mater. Sci. **30**, 153–182 (2005).
[26]B. Radisavljevic, A. Radenovic, J. Brivio, V. Giacometti, and A. Kis, Nat. Nanotechnol. **6**, 147–150 (2011).
[27]W. Park, J. Park, J. Jang, H. Lee, H. Jeong, K. Cho, S. Hong, and T. Lee, Nanotechnology **24**, 095202 (2013).
[28]G. Kline, K. K. Kam, R. Ziegler, and B. A. Parkinson, Sol. Energy Mater. **6**, 337–350 (1982).
[29]E. Gourmelon, O. Lignier, H. Hadouda, G. Couturier, J. C. Bernède, J. Tedd, J. Pouzet, and J. Salardenne, Sol. Energy Mater Sol. Cells **46**, 115–121 (1997).
[30]J. He, K. Wu, R. Sa, Q. Li, and Y. Wei, Appl. Phys. Lett. **96**, 082504 (2010).
[31]A. Azcatl, S. McDonnell, K. C. Santosh, X. Peng, H. Dong, X. Qin, R. Addou *et al.*, Appl. Phys. Lett. **104**, 111601 (2014).
[32]W. Kohn and L. J. Sham, Phys. Rev. **140**, A1133–A1138 (1965).
[33]P. Hohenberg and W. Kohn, Phys. Rev. **136**, B864–B871 (1964).
[34]G. Kresse and J. Hafner, Phys. Rev. B. **47**, 558–561 (1993).
[35]G. Kresse and J. Furthmuller, Phys. Rev. B. **54**, 11169–11186 (1996).
[36]J. P. Perdew, K. Burke, and M. Ernzerhof, Phys. Rev. Lett. **77**, 3865–3868 (1996).
[37]P. E. Blochl, Phys. Rev. B. **50**, 17953–17979 (1994).
[38]H. J. Monkhorst and J. D. Pack, Phys. Rev. B. **13**, 5188–5192 (1976).
[39]G. H. Diercksen and S. Wilson, *Methods in Computational Molecular Physics* (Springer, 1983).
[40]G. Mills, H. Jonsson, and G. K. Schenter, Surf. Sci. **324**, 305–337 (1995).

[This article is copyrighted as indicated in the article. Reuse of AIP content is subject to the terms at: http://scitation.aip.org/termsconditions. Downloaded to] IP: 139.179.2.116 On: Tue, 16 Jun 2015 14:11:18

[41]G. Henkelman, A. Arnaldsson, and H. Jonsson, Comput. Mater. Sci. **36**, 354–360 (2006).
[42]On the other hand, even energetically not favourable when compared to the ideal MoS_2, the resulting structure ($Mo_{16}S_{15}O_1$) can indicate the possibility of formation of stable molybdenum oxide (MoO_x) by convenient processes.
[43]W. Zhou, X. Zou, S. Najmaei, Z. Liu, Y. Shi, J. Kong, J. Lou, P. M. Ajayan, B. I. Yakobson, and J.-C. Idrobo, Nano Lett. **13**, 2615–2622 (2013).
[44]S. McDonnell, R. Addou, C. Buie, R. M. Wallace, and C. L. Hinkle, ACS Nano **8**, 2880–2888 (2014).
[45]B. H. Xu, B. Z. Lin, D. Y. Sun, C. Ding, X.-Z. Liu, and Z.-J. Xiao, Mater. Res. Bull. **42**, 1633–1639 (2007).

[This article is copyrighted as indicated in the article. Reuse of AIP content is subject to the terms at: http://scitation.aip.org/termsconditions. Downloaded to] IP: 139.179.2.116 On: Tue, 16 Jun 2015 14:11:18